Capability of SRTM C- and X-band DEM Data to Measure Water Elevations in Ohio and the Amazon

Brian Kiel, Doug Alsdorf, and Gina LeFavour

Abstract

We analyze Shuttle Radar Topography Mission (SRTM) water surface elevation data to assess the capacity of interferometric radar for future surface water missions. Elevations from three Ohio reservoirs and several Amazon floodplain lakes have standard deviations, interpreted as errors, that are smaller in C-band compared to X-band and are smaller in Ohio than in the Amazon. These trends are also evident when comparing water surface elevations from the Muskingum River in Ohio with those of the Amazon River. Differences are attributed to increased averaging in C-band compared to X-band, greater sensitivity to surface water motion in X-band, and generally larger off-nadir look angles in X-band. Absolute water surface elevations are greater in the C-band DEM for much of the two study areas and yield expected slope values. Height and slope differences are attributed to differing usage of geoids and ellipsoids. These SRTM measurements suggest the great possibility for space-based, laterally-spatial (2D) measurements of water surface elevations.

Introduction

The terrestrial branch of the water cycle is an important component of weather, climate, and water resource management. Discharge (Q) in river channels is a particularly appealing measurement because it represents a spatial and temporal integration of basin-wide hydrologic processes. Changes in water volumes stored (ΔS) in wetlands, lakes, and reservoirs serve to regulate the delivery of flow to downstream locations. For example, Coe (2000) used a continental-scale hydrologic mass-balance and transport model and found that the addition of a wetlands storage component reduced the model discharge output by an amount equal to approximately 50 percent of the observed Nile River annual discharge in the Sudan. Unfortunately, there is a paucity of Q and ΔS measurements in the non-industrialized and remote regions of the world (IAHS, 2001; Stokstad, 1999; Shiklomanov *et al.*, 2002). For example, the central Amazon contains two orders of magnitude fewer gauging stations than a similar sized area centered on Washington D.C., but the central Amazon incorporates two orders of magnitude greater flow. Therefore, the hydrology community is seeking methodologies capable of collecting global discharge and storage change measurements (Alsdorf *et al.*, 2003).

The primary objective of this paper is to demonstrate the potential of Version 1 Shuttle Radar Topography Mission (SRTM) data for use in hydrologic applications. Hydrologists, water resource managers, and engineers recognize the potential of remote sensing for acquiring the hydraulic measurements necessary for estimating Q and ΔS globally, and thus have formed a community proposing the *Wat*er *E*levation *R*ecovery satellite mission (WATER; Mognard *et al.*, 2005; Alsdorf *et al.*, 2005a and in Review). The WATER technological heritage is directly based on the highly successful SRTM and its C-band and X-band digital elevation models (DEMs). SRTM used two synthetic aperture radar (SAR) antennae attached to opposite ends of a 63 m boom to form an interferometric system operating at 20° to 60° look angles. WATER is proposed as a *Ka*-band *R*adar *IN*terferometer (KARIN) using two Ka-band SAR antennae at opposite ends of a 10 m boom operating at very near nadir with a maximum 4.5° look angle. WATER is designed to collect measurements of water surface elevations (h) and their spatial and temporal derivatives ($\partial h/\partial x$ and $\partial h/\partial t$) throughout a 120 km wide swath with complete global coverage every eight days.

SRTM is not only a technological heritage for WATER but also a baseline measurement by which we can assess the potential of remote sensing to collect measurements of h, $\partial h/\partial x$ and $\partial h/\partial t$. The C-band relative height errors of 5.5 m (90 percent level) reported by the Jet Propulsion Laboratory (JPL) SRTM mission team (Rodriguez, 2005) are for terrestrial land surfaces, not water surfaces. A first assessment of SRTM performance over water surfaces by LeFavour and Alsdorf (2005) has demonstrated that the C-band DEM height errors from the Amazon River channel are ± 5.51 m ($1\ \sigma$ level). Here, we build upon this initial effort by determining the h errors across a river about three orders of magnitude smaller than the Amazon and across flat reservoirs and lakes in both the C-band and X-band DEMs. These water bodies are located in the State of Ohio, poleward of the equatorial Amazon and thus should show improved errors given the greater number of data takes averaged in the SRTM C-band DEM. This is the primary reason for our selection of Ohio water bodies in addition to the Amazon Basin: we expect C-band coverage (and consequently error) to vary with latitude. However, given the acquisition patterns (Bammler, 1999), the Ohio X-band DEM should maintain height error characteristics similar to the Amazon X-band DEM.

Brian Kiel and Doug Alsdorf are with the Department of Geological Sciences, Ohio State University, Columbus, OH (kiel.14@osu.edu; alsdorf.1@osu.edu).

Gina LeFavour is with the Department of Geography, UCLA, Los Angeles, CA.

Photogrammetric Engineering & Remote Sensing
Vol. 72, No. 3, March 2006, pp. 000–000.

0099-1112/06/7203–0000/$3.00/0

The Ohio and Amazon Study Locations

The climate of Ohio, 40.0°N 83.0°W (Figure 1), is continental with a seasonal temperature range between a normal daily minimum of −6.5°C in January to a normal daily maximum of 29.6°C in July (all data from OARDC, 2005). Precipitation is highest in the Spring and Summer and ranges from a low monthly average in February of 5.6 cm to a high of 11.7 cm in July (snowfall reaches a monthly maximum of 22.4 cm in January). January and February 2000 mean temperatures were −2.4°C and 3.3°C, respectively. The study locations include three reservoirs that supply water for the city of Columbus (Figure 2) and the Muskingum River, a tributary to the Ohio River, draining over 19,500 km^2. Water elevations on the reservoirs are controlled by dams with small annual elevation ranges whereas the Muskingum hydrograph shows low flows of approximately 50 m^3/s in the Summer and Fall with high flows of approximately 400 m^3/s in the Winter and Spring (USGS, 2005).

The climate of the Amazon Basin (Figure 1) is a function of the south to north seasonal migration of the precipitation driven by the Intertropical Convergence Zone (ITCZ). The ITCZ, combined with the vast extent of the basin and water storage on the floodplains contribute to a damped and regular hydrograph of the Amazon main stem (Richey *et al.*, 1989a, Meade *et al.*, 1991). Differential timing of precipitation inputs causes the peak discharge of the Amazon main stem to vary only 2 or 3 times from that of the low flow discharge while discharge of individual tributaries can vary by a factor of 10 (Richey *et al*, 1989b; Meade, *et al.*, 1991). The hydrograph is further moderated by water stored seasonally on the floodplain. These floodplain waters exhibit hysteresis with slow discharge back into the main stem during the falling limb of the annual flood wave (Meade, *et al.*, 1991). The hydrograph of water stage at the Manaus gage on the Rio Negro, very near the confluence

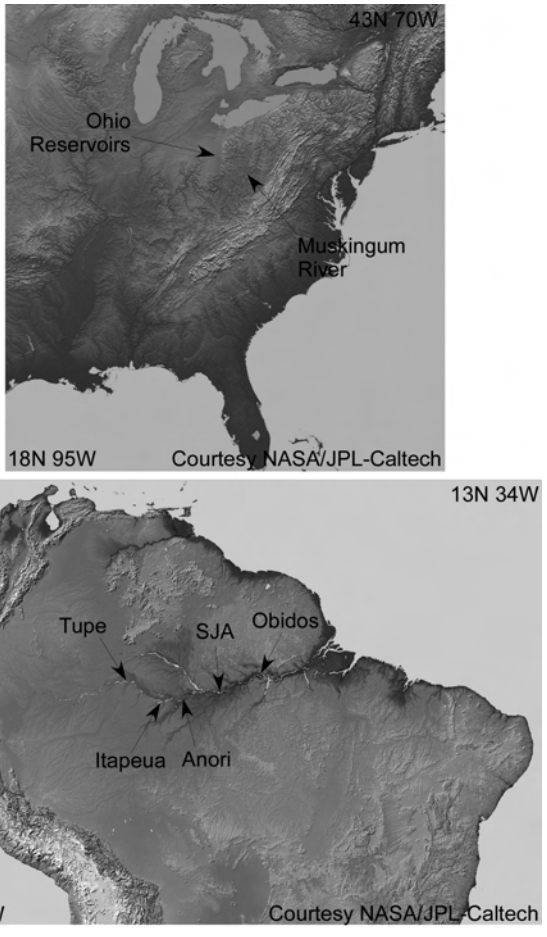

Figure 1. Study locations in the State of Ohio and the Amazon Basin. Background imagery is the C-band SRTM DEM. SJA = Sao Jose do Amatari.

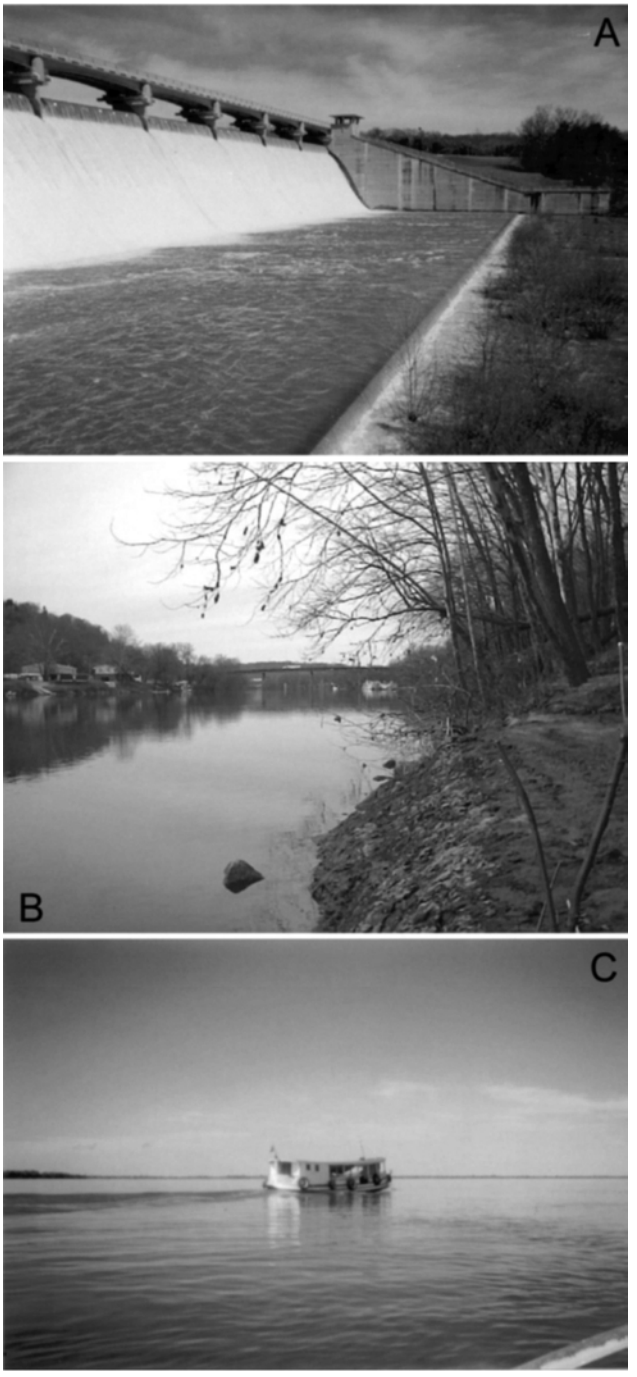

Figure 2. Photographs of study location reservoirs and rivers: (a) the dam on the Hoover Reservoir, (b) the Muskingum River, and (c) the Amazon River.

with the Amazon River, represents the only long-term record of stage in the entire Amazon Basin and clearly shows the regularity of the annual flood wave (Richey *et al.*, 1989b). Excluding eight low and two high flow years, the range for an average 12–22 February hydrograph is ±1.75 m, yet the overall stage change is 9.34 m at Manaus. The annual average discharge of the Amazon River is approximately 200,000 m^3/s (e.g., Meade *et al.*, 1991). Study locations include selected reaches of the Amazon mainstem and several floodplain lakes (Figures 1 and 2).

SRTM C- and X-band DEM Data

Factors that affect the surface water elevation accuracy of the SRTM DEMs include (a) the number of data takes, (b) look angles, and (c) the velocity of water flow. The C-band DEM near the equatorial Amazon River is constructed from two data takes whereas in Ohio (40.0°N) the convergence of the Shuttle orbits facilitated generally three to four data takes in the averaging used to build the C-band DEM. For spatially and temporally uncorrelated noise, the improvement in height accuracy is the square root of the number of samples. Thus, Ohio C-band DEM elevation accuracies should be 2.8 to 1.2 times improved compared to the Amazon (i.e., $\sqrt{4}/\sqrt{2}$ and $\sqrt{3}/\sqrt{2}$, respectively). In contrast, both the Ohio and Amazon X-band DEMs are built from one data take with the occasional exception where one ascending and one descending orbit cross. SRTM DEMs of the Ohio reservoirs, Muskingum River, and Amazon River and its floodplain lakes are presented in Plates 1, 2, and 3, respectively.

Microwave pulses are reflected specularly from water surfaces, thus far off-nadir viewing SAR geometries, such as those used by SRTM, result in low energy returns to the antennae. However, wave and wind action roughen water surfaces permitting stronger return, but generally only at the shorter C-and X-wavelengths (e.g., Smith and Alsdorf, 1998; longer L-wavelengths do not yield returns, e.g., Hess *et al.*, 1995). These returns are not necessarily consistent across space and time because wind and wave action that construct the radar scattering centers are not always similarly constant. Furthermore, when constructing a height value for a given C-band DEM pixel, the C-band look angles of 30° to 58° are mixed between the ascending and descending shuttle orbits with similarly mixed look directions. Because the X-band DEM used a nominal look angle of 52°, generally greater than the C-band acquisitions, X-band height accuracies are expected to be slightly poorer than those of C-band.

A significant source of error results from motion of the imaged water surface. The C- and X-band SAR antennae were displaced not only in the across track direction (63 m) but also in the along track direction (7 m). Along track interferometric SAR methods are well known for producing estimates of near shore oceanic wave velocities (e.g., Goldstein and Zebker, 1987; Goldstein *et al.*, 1989) and more recently for river flow velocities (Bjerklie *et al.*, 2005). An intriguing early result by Romeiser *et al.* (2005) uses the SRTM X-band interferometric phase and shows the first ever spaceborne estimate of river velocity. Essentially, the across and along track offsets yield an interferometric phase value that contains both an elevation measurement and a surface velocity,

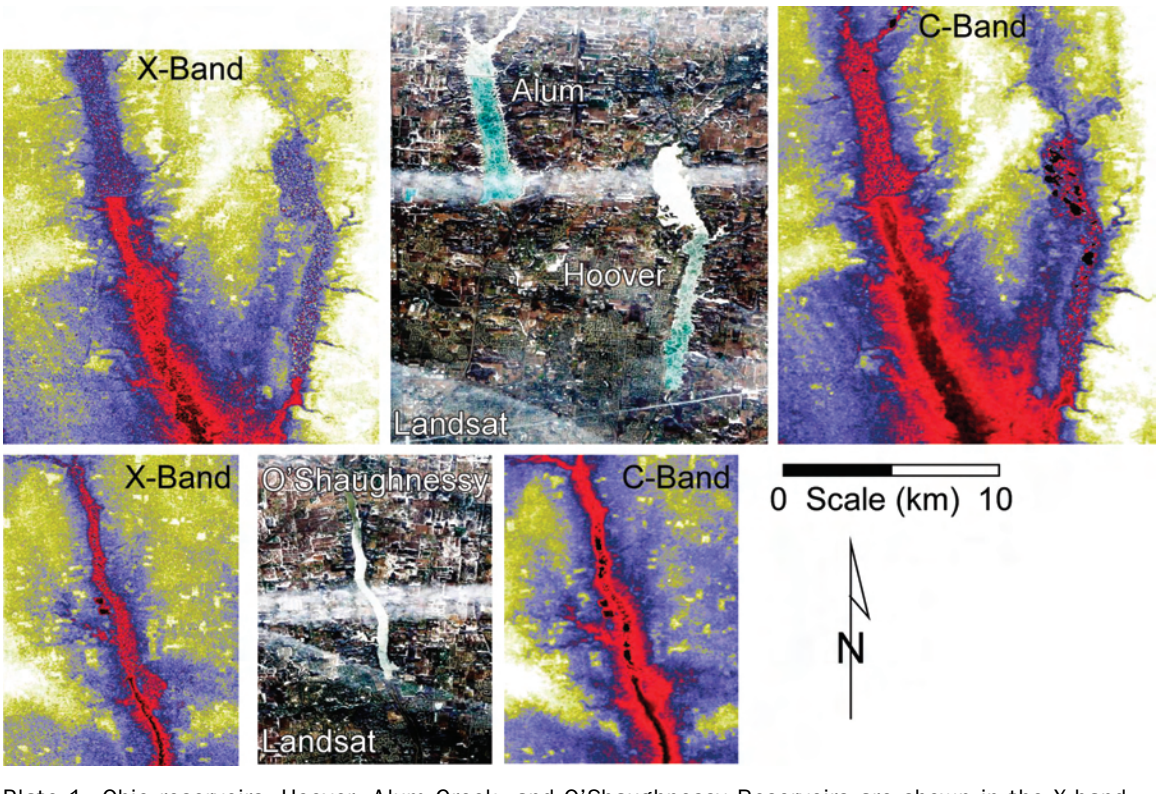

Plate 1. Ohio reservoirs. Hoover, Alum Creek, and O'Shaughnessy Reservoirs are shown in the X-band (left side) and C-band (right side) DEMs where elevations of 200 to 300 m are scaled from deep red to bright yellow, respectively. Center panels are true color Landsat imagery from 17 February 2000 (Courtesy of the Ohio View Project, **http://www.ohioview.org**).

respectively. Because the X-band wavelength is smaller than C-band, X-band is expected to yield a more accurate height measurement at the same look angle, but is also more sensitive to water motion. The multiple data takes and look directions of the C-band DEM help to reduce these errors induced by moving water surfaces, however segments of the X-band DEM constructed from singular acquisitions will be in error proportionately with the magnitude of water flow, wave motion, and wind action.

Precision and Accuracy of SRTM Water Surface Elevations

SRTM C- and X-band elevations over the study area water surfaces were extracted using overlay operations and hand drawn polygons. Water surface and terrestrial elevations are not always clearly differentiated in the SRTM DEMs resulting in shoreline definitions that could be erroneously marked by several nearby pixels when using only the elevation values. Instead, both optical Landsat and long microwave L-band SAR (JERS-1; Japanese Earth Resources Satellite) are overlaid on the SRTM DEMs to more clearly denote shorelines (e.g., Plates 1, 2, and 3; Rosenqvist *et al.*, 2000, 2002; Sheng and Alsdorf, 2005). Simple hand-drawn polygons defining the water body areas are used to extract the DEM water surface elevations (Figures 3, 4, and 5).

Since SRTM acquired data during 11–22 February 2000, we needed to determine whether the three Columbus reservoirs were frozen during this period. Potentially, ice coverage would be significant because ice scatters microwave energy differently than water and could thus generate false "water elevations." However, it is unlikely that the reservoir water surfaces in the 17 February 2000 Landsat image (Plate 1) are ice covered. In the five days prior to the Landsat acquisition, average daily air temperatures did not drop below freezing;

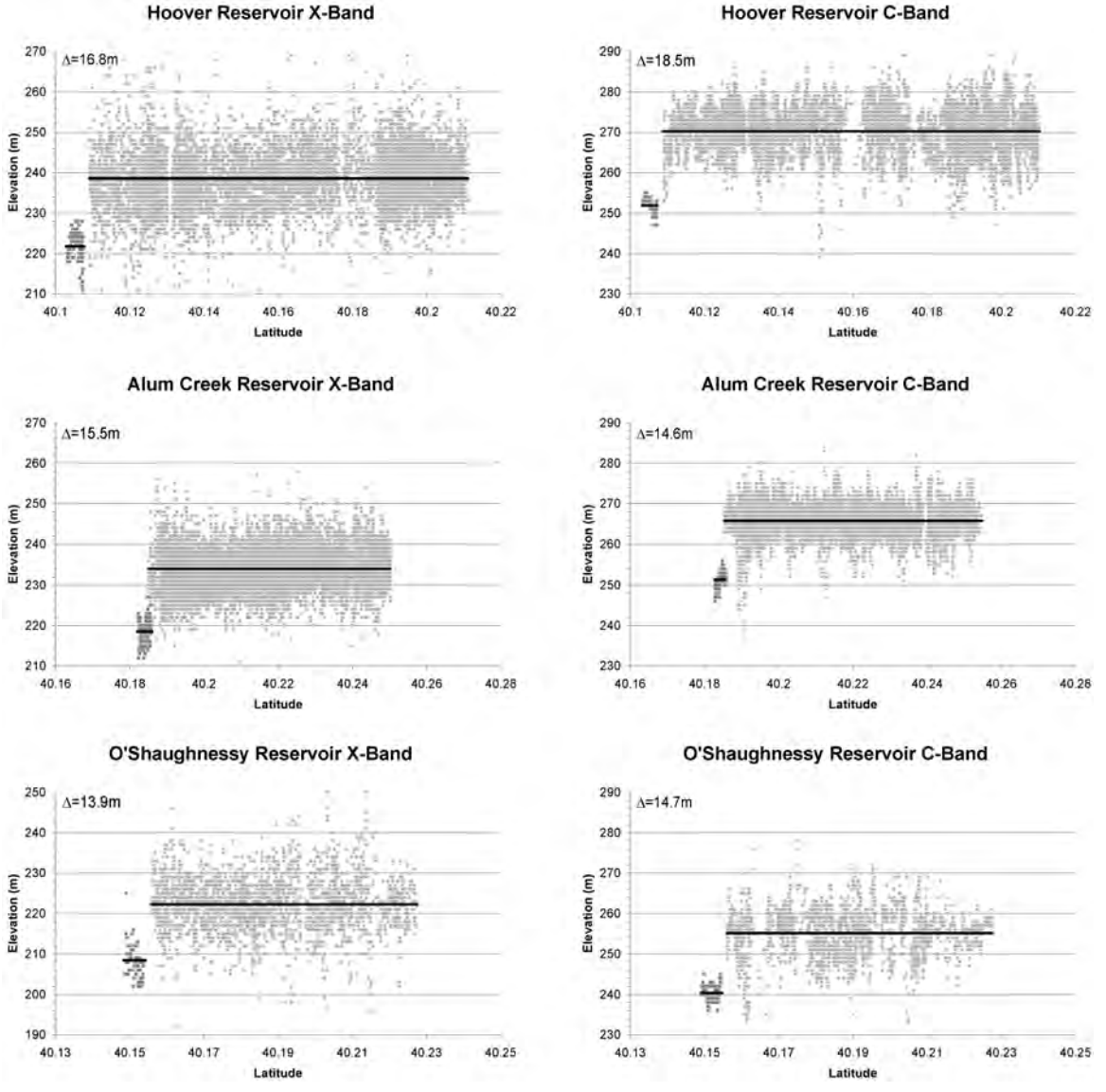

Figure 3. SRTM C- and X-band elevations from the Ohio reservoirs. Horizontal black lines are the average elevation from the above and below dam water surfaces. Water surface elevation differences across the dams are noted by Δ.

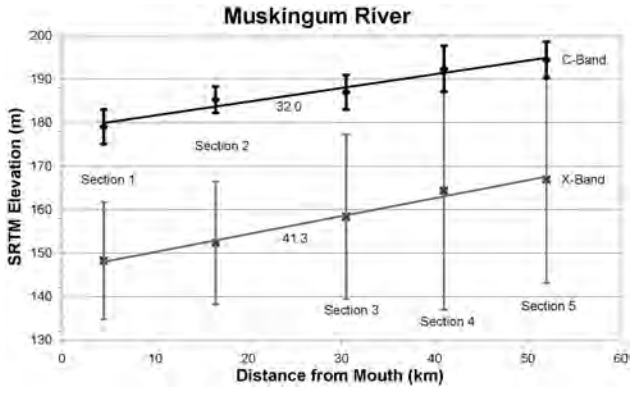

Figure 4. SRTM C- and X-band elevations along the Muskingum River. The five reaches are approximately 12 km long with the average elevation noted by the box (X-band) or black diamond (C-band). Linear fits to the data yield the average slopes indicated in cm/km. Error bars are 1 standard deviation above and 1 standard deviation below the plotted value.

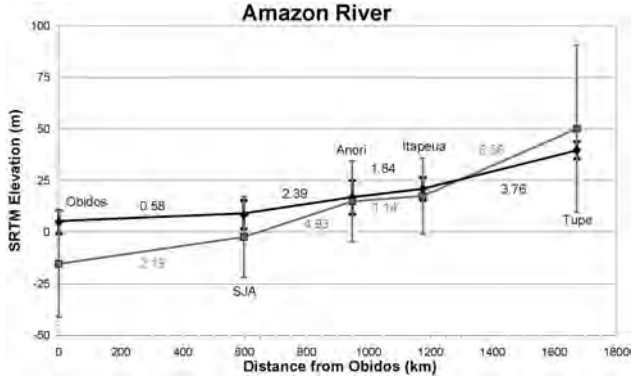

Figure 5. SRTM C- and X-band elevations along the Amazon River. The five reaches are approximately 50 km long with the average elevation noted by the box (X-band) or diamond (C-band). Linear fits to the data yield the average slopes indicated in cm/km. Error bars are 1 standard deviation above and 1 standard deviation below the plotted value.

the previous seven days average was above freezing at 33.9°F, and only when including the previous 16 days does the average equal freezing. In comparison, reservoir water surfaces in Landsat imagery of 31 December 1999 and 04 March 2000 (not shown) are clearly open water and air temperatures in the seven days prior to acquisitions averaged 28.1°F and 44.2°F, respectively. A reflectivity similar to Plate 1 was present in the 06 February 2005 Landsat image. The previous seven days average air temperature was 30.0°F, but from our field observations of the Alum Creek reservoir, no ice was present during this period in 2005. In sum, it is unlikely that ice was present during the SRTM timeframe.

Table 1 presents mean and standard deviation descriptions of the C- and X-band water surface elevations. The three Columbus, Ohio reservoirs and various Amazon floodplain lakes are all expected to have flat lying water surfaces, thus an assessment of the height error for the

TABLE 1. STANDARD DEVIATIONS AND AVERAGE ELEVATIONS OF OHIO AND AMAZON WATER SURFACES

Location	C-Band σ	X-Band σ	C-Band avg. h	X-Band avg. h
Ohio				
Hoover Reservoir	5.71	7.41	270.3	238.5
Hoover outlet	1.59	3.71	251.8	221.7
Alum Creek Reservoir	3.69	4.84	265.8	234.0
Alum Creek outlet	2.00	2.89	251.2	218.5
O'Shaughnessy Reservoir	6.00	7.04	255.0	222.2
O'Shaughnessy outlet	2.01	4.14	240.3	208.3
Muskingum R. Section 1	4.00	13.5	179.1	148.3
Muskingum R. Section 2	3.00	14.1	185.3	152.3
Muskingum R. Section 3	3.98	19.0	187.0	158.4
Muskingum R. Section 4	5.27	27.4	192.9	164.4
Muskingum R. Section 5	4.22	23.8	194.4	166.9
Amazon				
Amazon River at Obidos	5.59	25.7	5.03	−15.3
Amazon River at SJA	7.01	19.6	8.52	−2.25
Amazon River at Anori	8.25	19.6	16.9	15.0
Amazon River at Itapeua	5.56	18.4	21.1	17.6
Amazon River at Tupe	4.09	40.5	39.8	50.2
Floodplain Lakes, Anori	3.02	22.0		

Notes: All elevation and standard deviation values in meters. Number of samples varied from approximately 200 to approximately 10,000.

reservoirs and lakes is the standard deviation of the extracted SRTM elevations values. In contrast, the Muskingum and Amazon Rivers have natural slopes thus linear or polynomial trends were removed from the extracted elevations to make assessments of these height errors (LeFavour and Alsdorf, 2005).

As expected from the error characteristics previously discussed, X-band elevations all have greater standard deviations, hence errors, than the corresponding C-band locations (Table 1). The three Ohio reservoirs are located in a single X-band swath, with C-band elevation standard deviations showing a 1.2 to 1.3 improvement over these X-band values. Along the Muskingum River, standard deviations of the C-band DEM elevation values are markedly better by 3.4 to 5.6 times compared to those of the X-band DEM (Table 1). This difference is likely related to both the greater number of averaging swaths used in the C-band DEM and the greater sensitivity of X-band interferometric phase to water flow. Muskingum River sections 1, 2, and 3 are all located in two crossing X-band swaths, and thus have lower standard deviations compared to sections 4 and 5 which are located in a single swath (improvements are about the expected $\sqrt{2}$). Amazon floodplain lakes and the main river channel all have lower standard deviations at C-band compared to X-band (Table 1). At five different locations spread intermittently along approximately 2000 km of the Amazon River, the X-band DEM values have standard deviations at least twice that of the C-band DEM. X-band values are collected from single data takes, and with the exception of Tupe, the standard deviations are comparable with X-band values from the Muskingum River. As expected from the increased number of data takes over Ohio, compared to the Amazon, the mean standard deviation is improved by 1.5 times.

All C-band (JPL) elevations are referenced to the WGS84 EGM96 geoid and horizontally georeferenced to the WGS84 ellipsoid using a geographic projection. Unlike C-band, X-band (DLR, Deutschen Zentrum für Luft- und Raumfahrt) elevations are exclusively referenced to the WGS84 ellipsoid (Farr *et al.*, in review). Thus regional variability in the

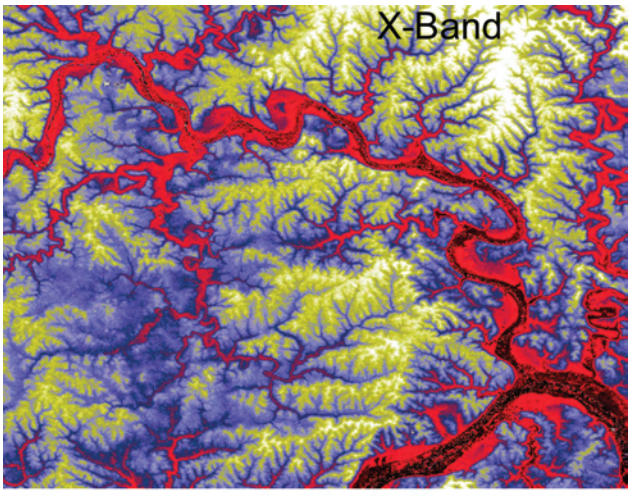

(a)

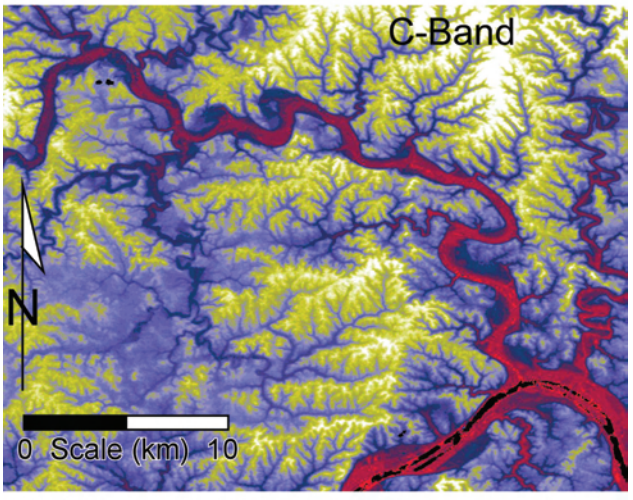

(b)

(c)

Plate 2. Muskingum River: (a) X-band and (b) C-band DEM elevations range from 150 m to 300 m and are scaled from deep red to bright yellow. Landsat true color image (c) is from 25 January 2000 (Courtesy of the Ohio View Project, **http://www.ohioview.org**).

Earth's shape is insufficiently accounted for by the X-band data. Since we are more concerned with data precision (variability) than with absolute accuracy, we did not attempt geoidal corrections to the X-band data. Consequently, X-band absolute elevations are clearly incorrect on the Amazon River downstream of Sao Jose do Amatari (SJA), where water surfaces are reported below sea level (Figure 5). X-band elevations are routinely lower than corresponding C-band elevations in both Ohio and the Amazon.

Here, water surface height accuracies are assessed by using river slopes and relative comparisons made above and below the three Ohio reservoir dams. Unfortunately, in-situ stream gauge data indicating water surface elevations in February 2000 are not available for any of the locations (discharge is available at some locations). Such comparisons would assume that a gauge and SRTM both used the same datum, which is unlikely given the heights listed for various gauges in Ohio (USGS, 2005). The dam at Hoover reservoir is 20.4 m high (Figure 2), the dam at Alum Creek Reservoir is 24.7 m, and at O'Shaughnessy Reservoir, the dam is 27.7 m. Fortunately, these dam heights are all greater than the elevation differences between reservoir water surfaces and the respective outlets (Figure 3). Use of the nonparametric Mann-Whitney test of population distribution (Davis, 1986; Hirsch *et al.*, 1993) and a 99 percent probability level (i.e., $\alpha = 0.01$) suggests that the elevation values above and below the dams are statistically separate. The water surface elevation differences at each reservoir compare well between C- and X-bands and are within 0.8 m to 1.7 m of each other. These differences from above and below the dams are local and not influenced by datum differences between the C- and X-band DEMs.

River slopes represent a regional difference in water heights and do show the effects of varying datums. Muskingum River slopes are not reported by the USGS; instead comparisons can be made between USGS reported velocities and SRTM-derived slopes using Manning's velocity equation (Albertson and Simons, 1964). Historic flow velocities on the Muskingum River range between 0.15 m/s and 2.0 m/s, with typical Winter and Spring stage flows of 0.5 to 1.5 m/s (USGS, 2005). Using USGS reported channel widths and depths (USGS, 2005) and Manning's roughness coefficient $n = 0.04$, the SRTM C- and X-band slopes in Figure 4 yield velocities of 0.7 to 2.0 m/s (1.3 m/s average) and 1.3 to 2.0 m/s (1.7 m/s average), respectively; thus, these SRTM water surface elevations are reasonable. On the Amazon River, slope comparisons can be made with estimates from Topex/POSEIDON radar altimetry. Birkett *et al.* (2002) used this altimetry data to investigate slopes and found none greater than 5 cm/km along approximately 4000 km of the Amazon mainstem. Within our study locations, their reported slopes were between 1 cm/km and 4 cm/km. This comparison suggests that the C-band slopes, and related water surface elevations, are more accurate than the X-band values. In particular, the Obidos to Tupe distribution of C-band slope magnitudes is very similar to that reported by Birkett *et al.* (2002) for a similar mid-rising water season (their data are from 1995 and 1996).

Conclusions

SRTM has provided the first ever spaceborne image based measurements of surface water elevations, thus it is both the technological and measurement heritage for the proposed WATER mission. Compared to X-band, the increased averaging, generally smaller look angles, and lower sensitivity to motion of the imaged surface in C-band has yielded improved accuracies of surface water elevations in both the Amazon and Ohio C-band DEMs. Because geoid and ellipsoid corrections differ in the Version 1 SRTM data, the absolute

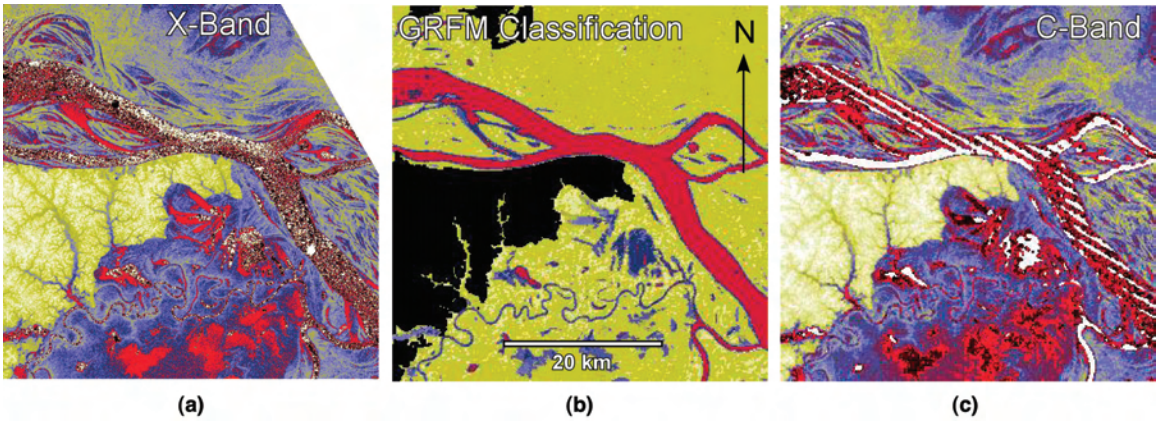

Plate 3. Amazon River at Tupe: (a) X-band and (c) C-band elevations range from 40 m to 100 m and are scaled from deep red to bright yellow. The Global Rain Forest Mapping (c) (GRFM; Rosenqvist *et al.* 2000 and 2002) mission mosaiced the Japanese Earth Resources (JERS-1) SAR data across the entire Amazon Basin and Hess *et al.* (2003) classified the SAR data such that open water is clearly delineated in the Amazon main channel (colored red). Examples of floodplain lakes are located approximately 5 km and approximately 20 km to the southwest.

elevations of the X-band DEM are typically lower than the corresponding C-band water surface values. The two studied rivers have steeper slopes in the X-band DEM. Local differences in water elevations from above and below three dams are similar in both the C- and X-band DEMs. We find that, while SRTM data are generally viable for hydrologic application, shortcomings such as the along-track antennae offset and the wide look-angle suggest the necessity of a new satellite mission (WATER) geared towards improved water elevation acquisition.

Acknowledgments

This research is funded by NASA's Terrestrial Hydrology program and their Solid Earth and Natural Hazards program. We thank both the JPL and DLR SRTM teams for their outstanding work to produce the DEMs. The GRFM mission generously supplied the JERS-1 mosaics used in the Amazon portions of this study. We also thank Dr. Chistopher Jekeli and Dr. Shin-Chan Han for their insight into relevant geodetic science.

References

Albertson, M.L., and D.B. Simons, 1964. Section 7: Fluid Mechanics, *Handbook of Applied Hydrology a Compendium of Water-resources Technology* (V.T. Chow, editor), McGraw-Hill, New York, 7.1–7.49.

Alsdorf, D.E., and D.P. Lettenmaier, 2003. Tracking fresh water from space, *Science*, (301):1485–1488.

Alsdorf, D., D. Lettenmaier, C. Vörösmarty, and the NASA Surface Water Working Group, 2003. The need for global, satellite-based observations of terrestrial surface waters, *EOS Transactions of AGU*, 84(269):275–276.

Alsdorf, D., E. Rodriguez, D. Lettenmaier, and J. Famiglietti, 2005a. WatER: The Water Elevation Recovery satellite mission, a response to the National Research Council Decadal Survey Request for Information, URL: http://www.geology.ohio-state.edu/water (last date accessed: 20 December 2005).

Alsdorf, D.E., E. Rodriguez, and D.P. Lettenmaier, In review. Measuring surface water from space, *Reviews of Geophysics*.

Bammler, R., (1999). The SRTM mission: A world-wide 30 m resolution DEM from SAR interferometry in 11 days, *Photogrammetric Week*, 145–154.

Birkett, C.M., L.A.K. Mertes, T. Dunne, M.H. Costa, and M. J. Jasinski, 2002. Surface water dynamics in the Amazon Basin: Application of satellite radar altimetry, *Journal of Geophysical Research*, 107(D20):8059.

Bjerklie, D.M., D. Moller, L. Smith, and L. Dingman, 2005. Estimating discharge in rivers using remotely sensed hydraulic information, *Journal of Hydrology*, (309):191–209.

Coe, M.T., 2000. Modeling terrestrial hydrological systems at the continental scale: Testing the accuracy of an atmospheric GCM, *Journal of Climate*, (13):686–704.

Davis, J.C., 1986. *Statistics and Data Analysis in Geology*, Second Edition, New York, John Wiley and Sons.

Farr, T.G., E. Caro, R. Crippen, R. Duren, S. Hensley, M. Kobrick, M. Paller, E. Rodriguez, P. Rosen, L. Roth, D. Seal, S. Shaffer, J. Shimada, J. Umland, and M. Werner, In review. The Shuttle Radar Topography Mission, *Reviews of Geophysics*.

Goldstein, R.M., T.P. Barnett, and H.A. Zebker, 1989. Remote sensing of ocean currents, *Science*, (246):1282–1285.

Goldstein, R.M., and H.A. Zebker, 1987. Interferometric radar measurement of ocean surface currents, *Nature*, (328):707–709.

Hirsch, R.M., D.R. Helsel, T.A. Cohn, and E.J. Gilroy, 1993. Statistical analysis of hydrologic data, *Handbook of Hydrology*, (D.R. Maidment, editor), New York, McGraw-Hill, 17.1–17.55.

Hess, L.L., J.M. Melack, E.M.L.M. Novo, C.C.F. Barbosa, and M. Gastil, 2003. Dual-season mapping of wetland inundation and vegetation for the central Amazon basin, *Remote Sensing of Environment*, 87(4):404–428.

Hess, L.L., J.M. Melack, S. Filoso, and Y. Wang, 1995. Delineation of inundated area and vegetation along the Amazon floodplain with SIR-C synthetic aperture radar, *IEEE Transactions on Geoscience and Remote Sensing*, (33):896–904.

IAHS Ad Hoc Group on Global Water Data Sets, 2001.Global water data: A newly endangered species, *EOS Transactions of AGU*, (82):54–58.

LeFavour, G., and D. Alsdorf, 2005. Water slope and discharge in the Amazon River using the Shuttle Radar Topography Mission digital elevation model, *Geophysical Research Letters*, (32):L17404 10.1029/2005GL023836.

Meade, R.H., J.M. Rayol, S.C. Da Conceicao, J.R.G. Natividade, 1991. Backwater effects in the Amzon River basin of Brazil, *Environmental and Geologic Water Sciences*, (18):105–114.

Mognard, N., and twenty-five contributors, 2005. WatER: The Water Elevation Recovery mission, a proposal to the Earth Explorer program of the European Space Agency, URL: http://www.

bafg.de/servlet/is/10614 (last date accessed: 20 December 2005).

OARDC, Ohio Agricultural and Research Development Center, 2005. URL: http://www.oardc.ohio-state.edu/centernet/weather.htm (last date accessed: 20 December 2005).

Richey, J.E., L.A.K. Mertes, T. Dunne, R.L. Victoria, B.R. Forsberg, A.C.N.S. Tancredi and E. Oliveira, 1998a. Sources and routing of the Amazon River flood wave, *Global Biogeochemical Cycles*, (3):191–204.

Richey, J.E., C. Nobre, and C. Desser, 1989b. Amazon River discharge and climate variability: 1903 to 1985, *Science*, (246):101–103.

Rodriguez, E., 2005. A Global Assessment of the SRTM accuracy, The Shuttle Radar Topography Mission – Data Validation and Applications Workshop, Reston, Virginia, 14–16 June, URL: http://edc.usgs.gov/conferecnes/SRTM/WorkshopProgram.html (last date accessed: 20 December 2005).

Romeiser, R., J. Sprenger, and D. Stammer, 2005. Global current measurements in rivers by spaceborne along-track InSAR, *Proceedings of IGARS '05*, unpaginated CD-ROM.

Rosenqvist, A., M. Shimada, B. Chapman, A. Freeman, G. DeGrandi, S. Saatchi, and Y. Rauste, 2000. The Global Rain Forest Mapping Project – A review, *International Journal of Remote Sensing*, (21):1375–1387.

Rosenqvist, A., M. Shimada, B. Chapman, L. Dutra, S. Saatchi, and O. Tanaka, 2002. The Global Rain Forest Mapping project: Introduction from the guest editors, *International Journal of Remote Sensing*, 23(7):1215.

Sheng, Y., and D. Alsdorf, 2005. Automated geo-referencing and ortho-rectification of Amazon Basin-wide SAR mosaics using SRTM DEM data, *IEEE Transactions on Geoscience and Remote Sensing*, 43(8):1929–1940.

Shiklomanov, A.I., R.B. Lammers, and C.J. Vörösmarty, 2002. Widespread decline in hydrological monitoring threatens Pan-Arctic research, *EOS Transactions of AGU*, (83):13–16.

Smith, L.C., and D.E. Alsdorf, 1998. Control on sediment and organic carbon delivery to the Arctic Ocean revealed with space-borne synthetic aperture radar: Ob' River, Siberia, *Geology*, (26):395–398.

Stokstad, E., 2005. Scarcity of Rain, Stream Gages Threatens Forecasts, *Science*, (285):1199, 1999.

USGS, United States Geological Survey, 2005., Gauge 03150000, URL: http://nwis.waterdata.usgs.gov/oh/nwis/ (last date accessed: 20 December 2005).